Macromolecules

ARTICLE

pubs.acs.org/Macromolecules

# Crystal Structure Analysis of Poly(L-lactic Acid) α Form On the basis of the 2-Dimensional Wide-Angle Synchrotron X-ray and Neutron Diffraction Measurements

Kaewkan Wasanasuk,[†] Kohji Tashiro,*[,†] Makoto Hanesaka,[†] Tokashi Ohhara,[‡] Kazuo Kurihara,[‡] Ryota Kuroki,[‡] Taro Tamada,[‡] Tomoji Ozeki,[§] and Tetsuo Kanamoto[⊥]

[†]Department of Future Industry-oriented Basic Science and Materials, Graduate School of Engineering, Toyota Technological Institute, Tempaku, Nagoya 468-8511, Japan

[‡]Research Unit for Quantum Beam Science Initiative, Japan Atomic Energy Agency, Tokaimura, Naka-gun, Ibaraki 319-1195, Japan

[§]Department of Chemistry and Materials Science, Graduate School of Science and Engineering, Tokyo Institute of Technology, Meguro, Tokyo 152-8551, Japan

[⊥]Faculty of Science, Tokyo University of Science, Ichigaya-Funagawara, Shinjuku-ku, Tokyo 162-0826, Japan

Supporting Information

**ABSTRACT:** The crystal structure of poly(L-lactic acid) (PLLA) α form has been analyzed in detail by utilizing the 2-dimensional wide-angle X-ray (WAXD) and neutron diffraction (WAND) data measured for the ultradrawn sample. The WAXD data were collected using a synchrotron-sourced high-energy X-ray beam of wavelength 0.328 Å at SPring-8, Japan and the WAND data were measured using a neutron beam of wavelength 1.510 Å with a cylindrical imaging-plate camera of BIX-3 system at Japan Atomic Energy Agency. The initial crystal structure model was extracted successfully by a direct method under the assumption of the space group $P2_12_12_1$ using about 700 X-ray reflections observed at −150 °C, the number of which was overwhelmingly large compared with the data reported by the previous other researchers and allowed us to perform more precise structural analysis. The crystal structure model obtained by the direct method was refined so that the best agreement between the observed and calculated integrated intensities was obtained or the reliability factor ($R$) became minimal: $R$ was 18.2% at −150 °C and 23.2% at 25 °C. The thus-obtained chain conformation took the distorted (10/3) helical form with $2_1$ helical symmetry along the chain axis. However, the symmetrically forbidden reflections 003, 007, 009 etc. were detected in a series of the 00$L$ reflections, requiring us to erase the $2_1$ screw symmetry along the molecular chain. By assuming the space group symmetry $P12_11$, the structural refinement was made furthermore and the finally obtained $R$ factor was 19.3% at −150 °C and 19.4% at 25 °C. Although the structural deviation from the $2_1$ screw symmetry was only slightly, this refined model was found to reproduce the observed reflection profiles well for all the layer lines. The thus X-ray-analyzed crystal structure was transferred to the WAND data analysis to determine the hydrogen atomic positions. The $R$ factor was 23.0% for the 92 observed reflections at 25 °C. The agreement between the observed and calculated layer line profiles was good. In this way the crystal structure of PLLA α form has been established on the basis of both the X-ray and neutron diffraction analyses.

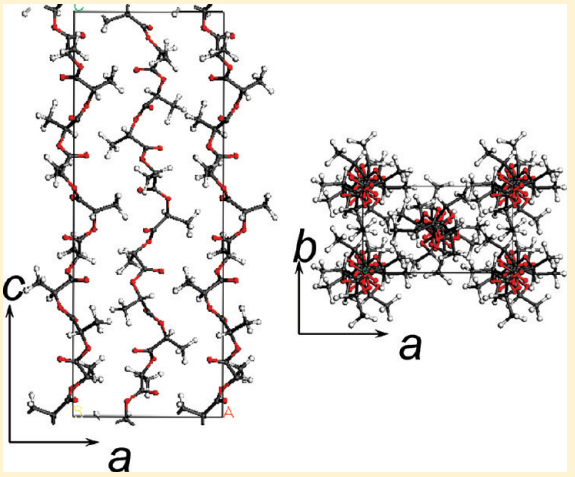


## INTRODUCTION

Poly(L-lactic acid) (PLLA, −[−$CH_2$−CH($CH_3$)−CO−O−]$_n$−) is one of the most typical environmentally friendly and biodegradable polymers, and has been utilized in a wide application field. However, PLLA has still some drawbacks about the physical properties compared with the other kinds of synthetic polymers like polyethylene, polypropylene, etc. For example, the Young's modulus of the bulk PLLA sample is 8 GPa and the tensioned film is easily broken at about 0.5 GPa.[1] Up to what maximal values can we increase the mechanical property of this polymer? In other words, what is the ultimate mechanical property? This information is important as a guiding principle for the development of PLLA sample with more excellent bulk property.[2−4] The theoretical estimation of the ultimate mechanical property of an ideal

**Received:** March 23, 2011
**Revised:** May 21, 2011
**Published:** July 20, 2011

crystalline state is made on the basis of lattice dynamical method, for example.[5,6] For this purpose we need the accurate atomic positions in the crystal lattice as well as the intra- and intermolecular interactions.[5,6] The X-ray (and neutron) structure analysis is one of the most powerful methods to obtain the atomic coordinates accurately.

PLLA exhibits several types of crystal modifications, α, α′, β, and γ phases and the stereocomplex between PLLA and PDLA.[7−19] In the present paper we focus our attention on the most stable α crystal form. In the long history of structure analysis of the α form, many papers tried at first to reveal the chain conformation as the starting information on the crystal structure analysis. For example, De Santis and Kovacs proposed a regular (10/3) helical chain on the basis of X-ray fiber pattern.[12] Brant et al. calculated the local conformational energy of an isolated chain and found the energy minima for the trans−gauche and gauche−gauche forms.[13] Okihara et al. proposed the (3/1) helical model on the basis of X-ray diffraction method, in particular, for the stereocomplex between PLLA and PDLA.[14] Kobayashi et al. proposed the (10/3) helices, the 2 chains of which were packed in the triclinic cell.[15] De Santis and Kovacs,[12] Hoogsteen et al.[16] and Kobayashi et al.[15] observed the odd-numbered 00*L* reflections in the X-ray fiber diagram, suggesting a distortion of chain conformation from the regular (10/3) helix as a result of intermolecular interactions between the neighboring chains. Alemán et al. measured the electron diffraction pattern of PLLA single crystal and proposed the space group of $P2_12_12_1$ as the most plausible packing mode of (10/3) helices.[17] This space group spontaneously causes the deformation of the uniform (10/3) helical chain to the conformation of $2_1$ helical symmetry along the chain axis. However, this space group cannot explain the odd-numbered 00*L* reflections. Kang et al. analyzed the infrared and Raman spectra of PLLA sample on the basis of normal modes calculation for the various conformational models of an isolated chain.[18] They assumed that the PLLA α form consists of the coexistence of the (3/1) and (10/3) helices. (Judging from the preparation conditions (annealed at 130 °C), their α form sample might contain the so-called α′ form or the conformationally disordered crystalline phase as proposed by Zhang et al.[8]) Sasaki et al.[19] analyzed the X-ray diffraction data of an oriented α form and refined the orthorhombic unit cell structure of the space group $P2_12_12_1$ in which the distorted (10/3) helical chains of $2_1$ screw symmetry were packed in an antiparallel mode along the chain direction, consistent with the structure proposed by Alemán et al. through the electron diffraction analysis.[17] Sasaki et al. speculated the observation of odd-numbered 00*L* reflections (003, 007 etc.) due to the disordered packing of the chains, but they did not give a concrete description.[19] In their paper, it is needed to notice the ratio between the total number of adjustable parameters and the number of the observed X-ray reflections. In their structural model, the 5 monomeric units are contained in a crystallographically asymmetric unit and the total number of variable parameters should be 101 [=5 atoms (C and O) × (3 coordinates +1 isothermal temperature factor) × 5 monomeric units +1 scale factor], even if all the hydrogen atoms were neglected and the temperature factors were assumed to be isotropic. The number of variables, 101, is almost the same order as the total number of reflections observed by them, 121. If the H atoms were taken into account and the anisotropic thermal parameters were introduced for the C and O atoms, the total number of variable to be determined is 306 [=5 atoms (C and O) × (3 coordinates +6 anisotropic thermal parameters) × 5 monomeric units +4 H atoms × (3 coordinates +1 isotropic thermal parameter) × 5 monomeric units +1 scale factor]. In this case it is impossible to get a unique answer of the crystal structure even if their X-ray data is fully utilized. The crystal structure proposed by Sasaki et al. seems to be essentially correct. But, in order to find the crystal structure with higher accuracy, we need to collect more number of the observed reflections far beyond the number of parameters.

Referring to these situations about the previously reported papers, we have to clear the several serious points in order to complete the structure analysis of PLLA α form with higher accuracy. One is to utilize the 2-dimensional X-ray diffraction data of as highly oriented and pure α form sample as possible, which may give us many spot-like reflections and should be useful for the separation of overlapped reflections. For this purpose the so-called ultradrawn fiber is the best at the present stage.[20] The second important point is to collect as many number of reflections as possible. As already mentioned above, the total number of observable reflections should be enough large far beyond the total number of parameters. As seen in the standard textbooks,[21−23] the X-ray diffraction can occur when a reciprocal lattice point is contacted with an Ewald sphere's surface, the radius of which is an inverse of wavelength of an incident X-ray beam. In order to increase the observable range of the X-ray diffractions as widely as possible, therefore, the X-ray beam with shorter wavelength is more preferable since the total number of reciprocal lattice points crossing the larger Ewald sphere surface increases correspondingly.[24]

To satisfy these experimental requirements, then we have performed the measurement of 2-dimensional X-ray diffraction data of the ultradrawn PLLA α form sample by using a synchrotron-sourced high-energy X-ray beam of quite short wavelength of 0.3282 Å. Usefulness of such high-energy X-ray beam was already confirmed in the crystal structure analyses of poly(oxymethylene)[25] and polyethylene.[26,27]

The third significant requirement necessary for getting the accurate crystal structure is to know the positions of hydrogen atoms. The three-dimensional anisotropy of the elastic constants is governed mainly by the intermolecular H···H interactions between the neighboring chains.[5] For example, the anisotropy of linear compressibility in the *ab* plane of orthorhombic polyethylene crystal is remarkably modified with and without the intermolecular H··H interactions.[28] The best agreement between the observed and calculated values is of course obtained when the H atoms are introduced in the crystal lattice. A usage of the so-called united atom model is impossible for the quantitative evaluation of anisotropic mechanical property. In this way the extraction of hydrogen atoms in the crystal lattice is indispensable for the theoretical estimation of anisotropic mechanical property of polymer crystals. An increment of the total number of observable X-ray reflections is useful also for this problem, as already checked for several types of polymer.[24,25] However, in general, the X-ray scattering power of hydrogen atom is quite low, making it difficult to find out the hydrogen atomic positions even for the single crystals of small molecules. The situation is more serious for the general polymer substances with quite limited number of X-ray reflections. In addition to the measurement of more number of X-ray diffraction data, then, we have challenged to collect the 2-dimensional wide-angle neutron diffraction (WAND) data for the ultradrawn and pure α form since the scattering power of hydrogen atoms by neutron beam is relatively large. As well-known, a preparation of fully deuterated polymer sample is ideal since the deuterium atom has a larger

neutron scattering cross-sectional area than that of the normal hydrogen atom. Some successful results were reported for polyethylene,[29] poly(oxymethylene),[25] poly(ethylene oxide),[30] *isotactic* polypropylene,[31] and *atactic* poly(vinyl alcohol)[32] where the fully deutereated samples were used. But the preparation of such fully deuterated polymer samples is quite difficult at the present stage. In a lucky case, however, even the normal hydrogen atom may be useful since it gives the negative peak in the atomic nucleus density map calculated by Fourier-transform of the observed neutron diffraction data, although the peak height is relatively low compared with the positive peak height of deuterium atom.[33] In the present paper, therefore, we applied also the hydrogenated ultradrawn α form sample used in the X-ray diffraction measurement to the neutron experiment.

In the present paper, we have challenged for the first time to perform the accurate crystal structure analysis of highly oriented and pure α form sample on the basis of 2-dimensional wide-angle X-ray and neutron diffraction data. We succeeded to collect about 700 X-ray reflections in the synchrotron experiment, which was far beyond the 121 reflections collected by Sasaki et al.[19] In addition to the X-ray diffraction data, the hydrogen atomic positions were also tried to determine on the basis of 2-dimensional neutron diffraction data. In the present paper, the results of the structure analysis will be described in detail for both the X-ray and neutron diffraction data. PLLA is one of the most promising biodegradable polymers. We hope the establishment of the accurate crystal structure would work as the most basically important information for the development of science and engineering of this polymer.

## EXPERIMENTAL SECTION

**Samples.** Ultradrawn sample of PLLA α form was prepared by the method reported by Kanamoto et al.[20] The total draw ratio was about 6. The sample was annealed at 170 °C for 1 h under tension to get the pure α form of higher crystallinity.

**Diffraction Measurements.** Wide-angle X-ray diffraction (WAXD) measurements were performed at a beamline BL04B2 of SPring-8, Japan with a high-energy X-ray source of 0.3282 Å wavelength. The Weissenberg-type cylindrical camera of 120 mm diameter equipped with an imaging plate was used as a 2-dimensional detector. The measurements were performed at 25 and −150 °C. The 00*L* reflections were measured by a transmission method using a Cu−Kα X-ray beam with a Rigaku TTR-III diffractometer at room temperature.

Wide-angle neutron diffraction (WAND) measurement was carried out at room temperature using a BIX-3 system (high resolution neutron diffractometer dedicated to biological macromolecules) built up in a JRR-3 reactor hall of the Japan Atomic Energy Agency, Tokaimura, Japan.[34] The monochromatized neutron beam of 1.510 Å wavelength was incident on the sample and the diffracted signals were detected using an imaging plate set in the cylindrical camera of 200 mm diameter. The sample specimen was a stack of ultradrawn PLLA α-form thick films and had a thickness of ca. 2.5 mm in total. The exposure time was about 40 h.

**Diffraction Data Analysis.** The thus-obtained 2-dimensional diffraction patterns were analyzed using a homemade software, by which the positions and integrated intensities of all the observed reflections were evaluated.[31] The peak positions of the observed reflections $(x, y)$ on the cylindrical camera were read out and transformed to the cylindrical coordinates $(\xi, \zeta)$ in the reciprocal lattice. The indexing of the observed reflections and the determination of the unit cell parameters were performed using these $(\xi, \zeta)$ data. The integrated intensity of each reflection was evaluated by summing up all the pixel data included in the encircled reflection spot, followed by the background correction. The overlapped reflections were separated by the curve fitting method. The thus-integrated intensities were corrected for Lorentz and polarization factors for the WAXD data, while the correction was made only for the Lorentz factor for the WAND data. No correction was made for the absorption effect for the synchrotron X-ray diffraction data. For the WAND data, the absorption coefficient was calculated by taking the large effect of light hydrogen atoms as a function of diffraction angle and used in the calculation of structure factors, where the neutron transmission was estimated to be ca. 15% by the existence of light H atoms, but the absorption coefficient was almost the same value in the diffraction angle range of the present WAND experiment.[35] The absolute value of the structure factor $|F(hkl)|$ was calculated for each reflection by taking the multiplicity into account. The layer line profiles were extracted from the observed 2-dimensional X-ray diffraction diagram by integrating the reflections over a certain width along each layer line.

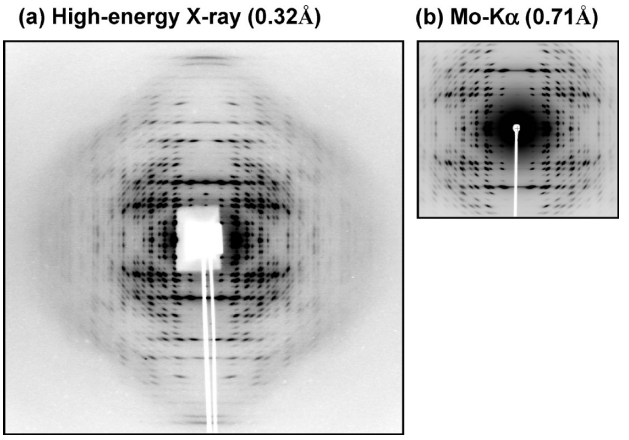


**Figure 1.** Wide-angle X-ray diffraction diagrams of ultradrawn PLLA α form taken at 25 °C with (a) a high-energy synchrotron X-ray beam and (b) Mo Kα X-ray beam. The cylindrical cameras were used. The draw axis is in the vertical direction.

**Structure Analysis.** The unit cell parameters were determined by indexing all the observed reflections. A set of data, *hkl* and $|F(hkl)|$, was transferred to the software of crystal structure analysis. For the calculation of diffraction intensities, a software WINGX (version 1.80.05) was utilized.[36] The direct method was applied to find out the initial model by using a SHELXS-86.[37] The model was refined with SHELXL-97 software on the basis of a full matrix least-squares method.[38] In the refinement procedure, the fractional coordinates and anisotropic temperature factors of carbon and oxygen atoms were varied at first, and then the hydrogen atomic positions were tried to extract from the 3-dimensional Fourier maps calculated using the observed structure factors ($F_o$) as well as the differential Fourier maps or the so-called $F_o - F_c$ map. But this trial was not made successfully, and then the H atoms were added to the carbon atoms using the standard geometry. The reliability factor was calculated as a measure of reliability of the structure analysis, which is defined as below.

$$R = \sum \left| |F_o(hkl)| - |F_c(hkl)| \right| / \sum |F_o(hkl)|$$

where $|F_o(hkl)|$ and $|F_c(hkl)|$ are, respectively, the absolute values of the observed and calculated structure factors. The summation was made for all the reflections used in the structural refinement.

## RESULTS AND DISCUSSION

**WAXD Structure Analysis.** *[Basic Crystal Structure].* The WAXD patterns measured for the ultradrawn PLLA sample are

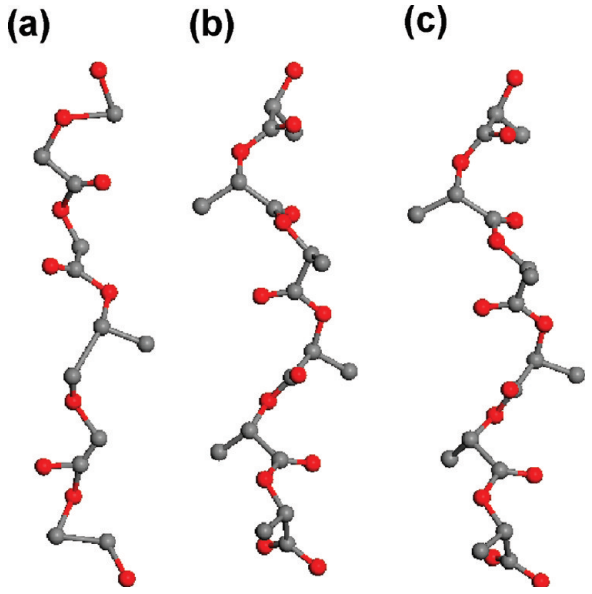


**Figure 2.** Chain conformations of PLLA α form: (a) a chain structure derived by a direct method, (b) a $2_1$ helix and (c) a finally determined chain without any symmetry along the chain axis. The data taken at −150 °C were used in this example.

reproduced in Figure 1, where part a is the data taken with a synchrotron high-energy beam of 0.3282 Å wavelength at 25 °C and part b is the data with a Mo Kα X-ray beam of 0.7107 Å in the laboratory. The WAXD pattern was also measured at −150 °C, which is not given here. In the comparison of the synchrotron data with that of Mo Kα beam, the tremendously large number of reflections is detected in the former case. After the separation of the overlapped reflections, the 692 reflections were collected in total at −150 °C and the 555 reflections at 25 °C. In the structure analysis reported by Sasaki et al., the 121 reflections were collected using a Cu Kα beam at room temperature.[19]

All the observed reflections were indexed successfully using an orthorhombic unit cell, the parameters of which are

$$\begin{aligned} 25\ ^\circ\mathrm{C} \quad a &= 10.683 \pm 0.001\ \text{Å}, \\ b &= 6.170 \pm 0.001\ \text{Å}, \\ c\ (\textit{fiber axis}) &= 28.860 \pm 0.004\ \text{Å} \end{aligned}$$

$$\begin{aligned} -150\ ^\circ\mathrm{C} \quad a &= 10.535 \pm 0.001\ \text{Å}, \\ b &= 6.170 \pm 0.001\ \text{Å}, \\ c\ (\textit{fiber axis}) &= 28.838 \pm 0.004\ \text{Å} \end{aligned}$$

The space group $P2_12_12_1$-$D_2^4$ was found to satisfy the extinction rules ($h00$ for odd $h$ and $0k0$ for odd $k$). The $00L$ reflections were, approximately speaking, consistent with this space group, but the detailed discussion will be made in a later section.

In order to obtain an initial model necessary for the structural refinement, the direct method was applied on the basis of the observed reflections.[36,37] Generally speaking, the direct method is actually impossible to apply to most of polymer materials because of small number of the observed broad X-ray reflections. But, some successful results were reported for the X-ray structure analysis of crystalline polymers giving enough number of the observed reflections such as orthorhombic polyethylene, trigonal

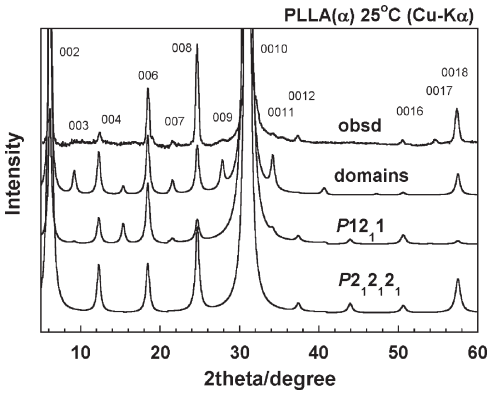


**Figure 3.** Comparison of the observed $00L$ reflection profile with the calculated curves for both of $P2_12_12_1$ and $P2_12_11$ models. The data were obtained at room temperature using Cu Kα X-ray beam in a transmission mode.

polyoxymethylene, *isotactic* poly(butane-1) form I, *etc.*[24,25] Since the total number of the observed reflections was about 700 at −150 °C in the present case of PLLA α form, the direct method was applied as a trial. Figure 2a shows the thus-obtained chain structure model, in which the skeletal chain atoms and some side-group atoms were found out. However, the chain conformation was not very reasonable judging from the stereochemical point of view. Starting from this initial model, the carbon and oxygen atomic positions were refined so that the calculated reflection intensities were in as good agreement with the observed values as possible, where the fractional coordinates ($x$, $y$, $z$) and anisotropic temperature factors ($U_{aniso}$) were modified as the parameters. Since some bond lengths were not reasonable, then the constrained conditions were introduced for the C−C and C−O bond lengths: C−$CH_3$, 1.54 Å; C(=O)−O, 1.46 Å; C−O, 1.31 Å; C(=O)−C, 1.53 Å; C=O, 1.20 Å. As a trial, the hydrogen atoms were searched in the $F_o$ and $F_o - F_c$ Fourier maps. But, only a few hydrogen atoms were extracted because even the observed 692 reflections were small in number for the unique determination of all the atoms in the unit cell. Then the hydrogen atoms were added using the standard geometry of C−H = 1.095 Å, ∠CCH = 109.5°, and ∠HCH = 109.5°. After the refinement the finally evaluated $R$ factor was 18.2% for the reflection data at −150 °C and 23.2% at 25 °C. Figure 2b shows the thus obtained chain conformation with the $2_1$ helical symmetry along the chain axis. This structure model is similar to that reported by Sasaki et al.[19]

*Introduction of Conformational Disorder.* The thus-analyzed crystal structure seems reasonable judging from the geometry of bond lengths, bond angles and torsional angles of the skeletal chains. But at this stage, however, we need to consider the two additional problems to be solved for the further refinement of the structure. One problem is relatively poor reproduction of the observed layer line profiles. The constrained least-squares method gives the structure which can minimize the total error between the observed and calculated integrated intensities or it gives the structure with the lowest $R$ factor. But, the $R$ factor is only a measure of the agreement between the observed and calculated values of the *integrated* X-ray reflection intensities. The integration over a certain range of reflection spots may eliminate the characteristic feature of the reflection profile. That is to say, the lowest $R$ factor is not necessarily a guarantee for the perfect reproduction of the observed *reflection profiles* themselves. Another problem is about the $00l$ reflections. Figure 3 shows a series

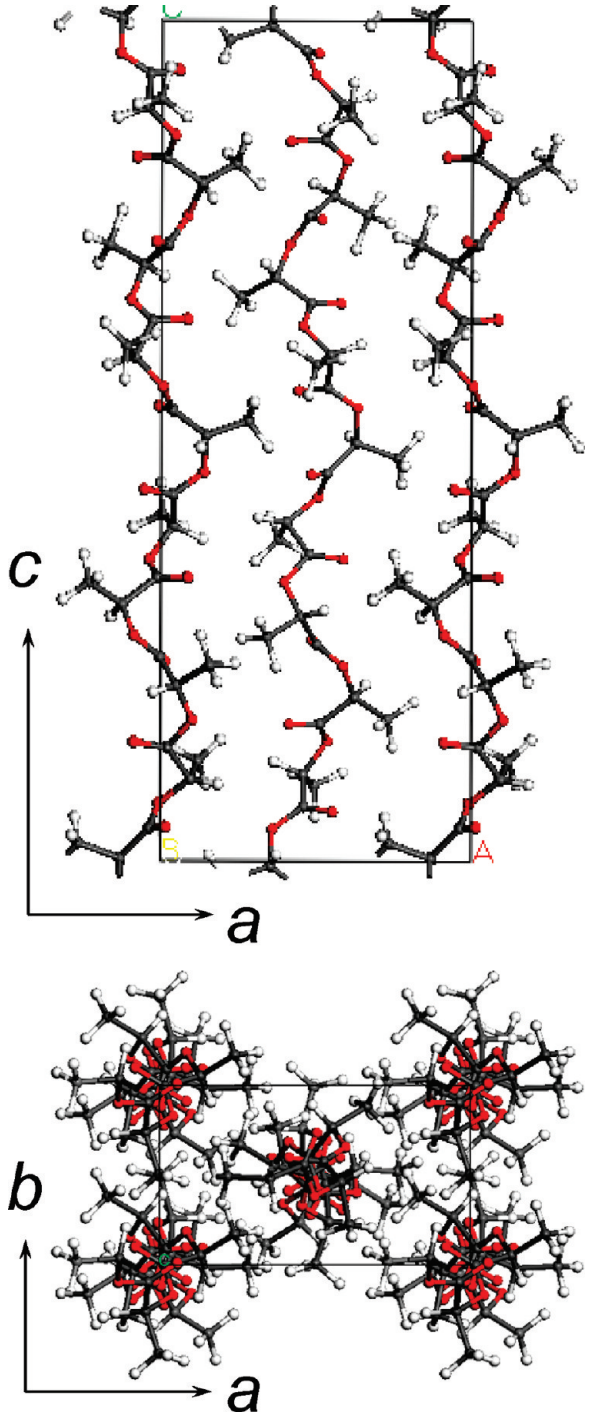


**Figure 4.** Finally determined crystal structure of PLLA α form. No symmetry is existent along the chain axis under the space group $P12_11$. The adjacent chains are packed upward and downward along the chain axis.

of X-ray 00*L* reflections of PLLA α form measured in a transmission mode. The even-numbered reflections of 002, 004, 006 and so on were detected clearly, supporting the $2_1$ screw symmetry along the chain axis. At the same time, however, some odd-numbered 00*l* reflections (003, 007, 009, ...) were also detected, although the intensity was not very high compared with that of the even-numbered reflections. The space group $P2_12_12_1$ had been assumed in the crystal structure analysis described in the preceding section, but an observation of these odd-numbered 00*l* reflections cannot be ignored. Sasaki et al. ascribed these observations to the disorder in chain packing mode,[19] but our calculation of 00*L* reflection intensities by introducing the chain packing disorder did not give any odd-numbered reflections *as long as the molecular chains keep the* $2_1$ *helical symmetry rigidly*. We needed to erase this symmetry along the chain axis. As a result, the orthorhombic symmetry of the unit cell must be reduced to the monoclinic or even the triclinic system with the orthogonal shape ($\alpha = \beta = \gamma = 90°$). Of course, the structure analyzed in the preceding section is essentially correct. We need to keep the spatial relation between the adjacent upward and downward helical chains in the orthogonal unit cell. As a tentative model, therefore, we applied the space group $P12_11$ by taking these situations into consideration. The unit cell is now that of monoclinic symmetry with the orthogonal shape. A pair of asymmetric units of the 5 monomeric units along the chain axis become one larger asymmetric unit containing the 10 monomeric units. That is to say, all the skeletal torsional angles are now symmetrically independent. The constrained least-squares method was applied to this structural model and the final *R* factor was 19.3% at −150 °C and 19.4% at 25 °C. The thus-obtained crystal structure (−150 °C) is shown in Figure 4. This crystal gives a good reproduction of the observed layer line profiles as shown in Figure 5, parts a and b, at −150 and +25 °C, respectively, where the profiles were calculated using a software Cerius[2] (version 4.6, Accelrys Inc., the crystallite size of 100 × 100 × 100 Å$^3$ and the lattice stains of 0.2% x 0.2% x 0.2%). The atomic fractional coordinates are listed in Table 1, parts a and b, for −150 and +25 °C, respectively. The anisotropic temperature factors are given as a Supporting Information. The comparison between the calculated and observed structure factors is also given as a Supporting Information.

The skeletal torsional angles of a single chain are compared among the uniform helix, the $2_1$ helix and the finally derived helical model without any symmetry as shown in Table 2 and in Figure 2c. The torsional angles are not very seriously deviated from the $2_1$ helical form. Besides the two groups of five monomeric units along the chain axis show the relatively similar values to each other, suggesting that the molecular chains might be assumed to take the helical conformation of $2_1$ screw symmetry in the first approximation. More strictly speaking, however, the molecular chain is deviated more or less from the uniform (10/3) helix and loses the $2_1$ screw symmetry also, although the structural deformation is not very serious. The similar situation was observed for the cases of poly(ethylene oxide)[39] and polyoxymethylene.[25,40−44] In the former case the helical chain conformation is deformed from the regular (7/2) form and without any symmetry. In the case of polyoxymethylene, the (9/5) helix is generally and approximately accepted but the molecular chain conformation is (29/16) helix, which can give better agreement between the observed and calculated X-ray intensities, and does not have any symmetry along the chain axis. The case of PLLA chain can be summarized in the following way: the molecular chain is assumed in an approximation to take the deformed (10/3) helical form with $2_1$ screw symmetry along the chain axis, but, according to the more accurate analysis using 600−700 X-ray reflections, the chain is deformed furthermore and loses any symmetry along the chain axis although the magnitude of structure deviation is not very serious.


dx.doi.org/10.1021/ma2006624 |*Macromolecules* 2011, 44, 6441–6452

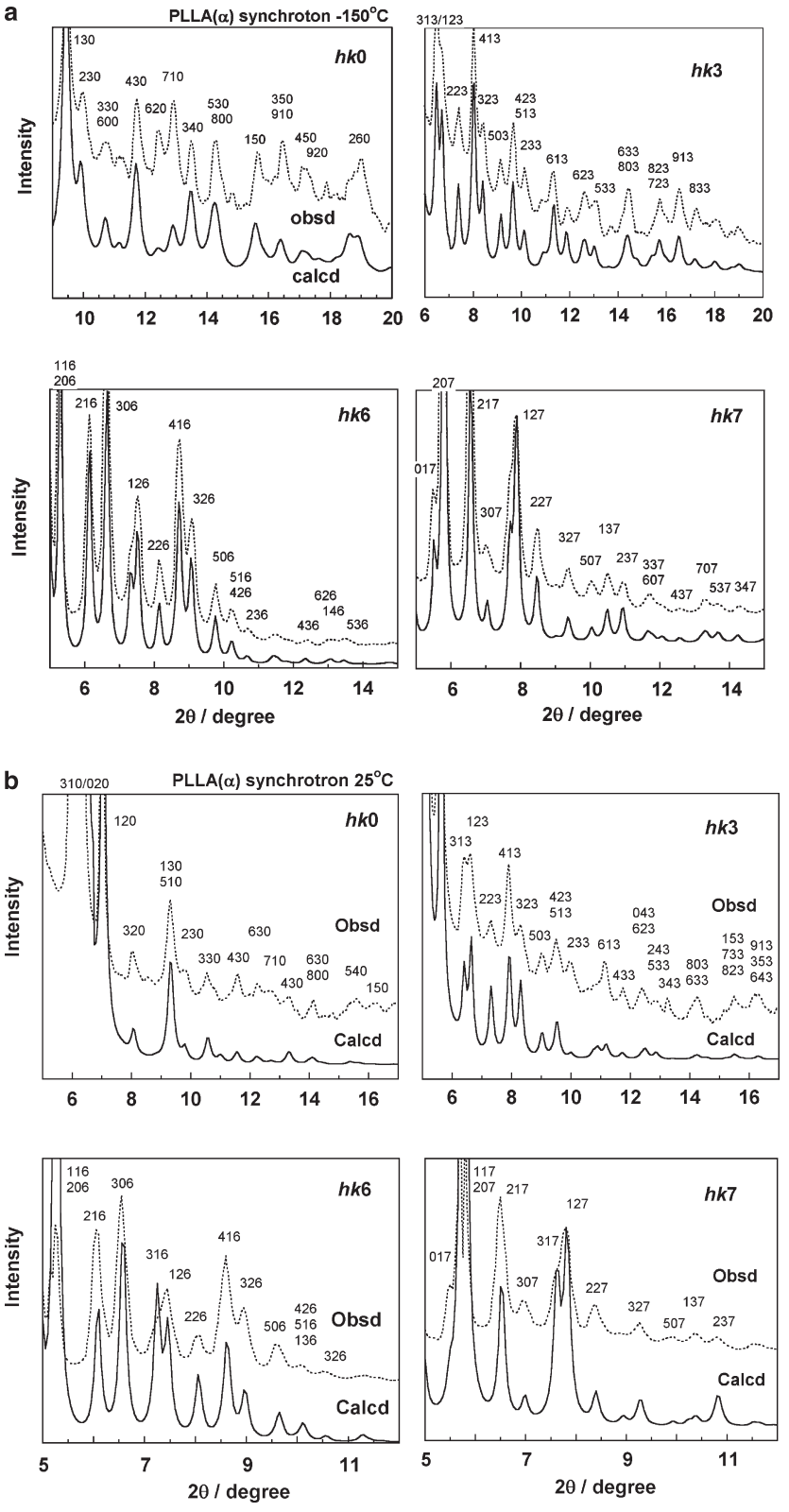


**Figure 5.** Comparison between the observed (dotted line) and calculated (solid line) X-ray diffraction profiles of PLLA α form for the several layer lines: (a) −150 °C and (b) +25 °C.

The 00*l* reflection profile was also calculated for the thus-determined crystal structure and compared with the observed one as shown in Figure 3, where the odd-numbered reflections are detected in addition to the even-numbered reflections. The tendency is reproduced fairly well, but not very perfect. Of course, the structure given in Table 1 and Figure 4 might be


dx.doi.org/10.1021/ma2006624 |*Macromolecules* 2011, 44, 6441–6452

Table 1. Atomic Fractional Coordinates and Thermal Parameters of PLLA α Form Analyzed at (a) − 150 °C and (b) 25 °C[a,b]

| | −150 °C | | | | | −150 °C | | | |
|---|---|---|---|---|---|---|---|---|---|
| (a) | $x$ | $y$ | $z$ | $U_{eq}$/Å$^2$ | | $x$ | $y$ | $z$ | $U_{eq}$/Å$^2$ |
| C1(1) | 0.0513 | −0.2524 | −0.1097 | 0.014(1) | C1(10) | −0.1303 | 0.0395 | 0.8002 | 0.009(1) |
| C2(1) | 0.0312 | −0.4890 | −0.0944 | 0.029(2) | C2(10) | −0.2289 | 0.1595 | 0.8293 | 0.050(3) |
| C3(1) | 0.0311 | −0.0976 | −0.0690 | 0.029(2) | C3(10) | −0.0149 | −0.0196 | 0.8290 | 0.050(3) |
| O4(1) | −0.0527 | 0.0324 | −0.0658 | 0.033(1) | O4(10) | 0.0787 | 0.0888 | 0.8315 | 0.020(1) |
| O5(1) | 0.1415 | −0.0983 | −0.0435 | 0.020(2) | O5(10) | −0.0425 | −0.1948 | 0.8529 | 0.025(2) |
| C1(2) | 0.1368 | 0.0365 | −0.0020 | 0.045(2) | H1(1) | 0.1455 | −0.2331 | −0.1224 | 0.02(1) |
| C2(2) | 0.2698 | 0.0290 | 0.0189 | 0.016(2) | H2(1) | 0.0569 | −0.5971 | −0.1220 | 0.13(4) |
| C3(2) | 0.0360 | −0.0482 | 0.0314 | 0.043(2) | H3(1) | −0.0650 | −0.5138 | −0.0853 | 0.05(2) |
| O4(2) | 0.0004 | −0.2336 | 0.0311 | 0.028(1) | H4(1) | 0.0889 | −0.5221 | −0.0647 | 0.05(2) |
| O5(2) | 0.0045 | 0.1179 | 0.0576 | 0.019(2) | H1(2) | 0.1148 | 0.2006 | −0.0118 | 0.05(2) |
| C1(3) | −0.0836 | 0.0553 | 0.0941 | 0.048(2) | H2(2) | 0.3374 | 0.0621 | −0.0081 | 0.15(4) |
| C2(3) | −0.1308 | 0.2680 | 0.1156 | 0.025(2) | H3(2) | 0.2870 | −0.1298 | 0.0334 | 0.04(2) |
| C3(3) | −0.0183 | −0.0784 | 0.1318 | 0.017(1) | H4(2) | 0.2775 | 0.1501 | 0.0458 | 0.05(2) |
| O4(3) | 0.0935 | −0.1015 | 0.1363 | 0.030(1) | H1(3) | −0.1619 | −0.0348 | 0.0804 | 0.08(2) |
| O5(3) | −0.0967 | −0.1670 | 0.1614 | 0.052(3) | H2(3) | −0.1854 | 0.3547 | 0.0903 | 0.02(2) |
| C1(4) | −0.0484 | −0.2685 | 0.2035 | 0.030(1) | H3(3) | −0.0526 | 0.3664 | 0.1261 | 0.09(3) |
| C2(4) | −0.1565 | −0.3935 | 0.2266 | 0.041(2) | H4(3) | −0.1883 | 0.2325 | 0.1452 | 0.21(5) |
| C3(4) | 0.0233 | −0.0906 | 0.2301 | 0.063(3) | H1(4) | 0.0184 | −0.3845 | 0.1899 | 0.04(2) |
| O4(4) | −0.0127 | 0.0957 | 0.2310 | 0.043(12) | H2(4) | −0.1965 | −0.5051 | 0.2022 | 0.14(4) |
| O5(4) | 0.0975 | −0.1706 | 0.2625 | 0.051(2) | H3(4) | −0.2266 | −0.2808 | 0.2381 | 0.09(3) |
| C1(5) | 0.1324 | −0.0392 | 0.3024 | 0.040(1) | H4(4) | −0.1215 | −0.4822 | 0.2559 | 0.15(4) |
| C2(5) | 0.2306 | −0.1687 | 0.3298 | 0.038(2) | H1(5) | 0.1761 | 0.1030 | 0.2878 | 0.08(2) |
| C3(5) | 0.0132 | 0.0278 | 0.3281 | 0.031(2) | H2(5) | 0.3070 | −0.2119 | 0.3068 | 0.05(2) |
| O4(5) | −0.0778 | −0.0852 | 0.3340 | 0.031(2) | H3(5) | 0.1884 | −0.3161 | 0.3431 | 0.05(2) |
| O5(5) | 0.0467 | 0.2023 | 0.3514 | 0.038(2) | H4(5) | 0.2654 | −0.0718 | 0.3582 | 0.05(2) |
| C1(6) | −0.0464 | 0.2553 | 0.3888 | 0.033(2) | H1(6) | −0.1390 | 0.2393 | 0.3746 | 0.09(3) |
| C2(6) | −0.0254 | 0.4894 | 0.4055 | 0.071(3) | H2(6) | −0.0328 | 0.6000 | 0.3769 | 0.12(3) |
| C3(6) | −0.0302 | 0.0991 | 0.4297 | 0.037(2) | H3(6) | 0.0663 | 0.5026 | 0.4207 | 0.09(3) |
| O4(6) | 0.0550 | −0.0268 | 0.4346 | 0.036(2) | H4(6) | −0.0946 | 0.5291 | 0.4312 | 0.05(2) |
| O5(6) | −0.1390 | 0.1001 | 0.4560 | 0.035(2) | H1(7) | −0.1123 | −0.2016 | 0.4875 | 0.16(4) |
| C1(7) | −0.1364 | −0.0378 | 0.4973 | 0.030(2) | H2(7) | −0.3357 | −0.0832 | 0.4923 | 0.07(2) |
| C2(7) | −0.2690 | −0.0399 | 0.5186 | 0.058(3) | H3(7) | −0.2901 | 0.1191 | 0.5317 | 0.04(2) |
| C3(7) | −0.0370 | 0.0479 | 0.5311 | 0.052(3) | H4(7) | −0.2720 | −0.1559 | 0.5463 | 0.05(2) |
| O4(7) | 0.0015 | 0.2320 | 0.5313 | 0.021(1) | H1(8) | 0.1595 | 0.0404 | 0.5803 | 0.01(1) |
| O5(7) | −0.0021 | −0.1077 | 0.5597 | 0.046(2) | H2(8) | 0.1782 | −0.3576 | 0.5872 | 0.20(5) |
| C1(8) | 0.0853 | −0.0510 | 0.5967 | 0.033(2) | H3(8) | 0.0674 | −0.3556 | 0.6320 | 0.04(2) |
| C2(8) | 0.1400 | −0.2645 | 0.6153 | 0.058(3) | H4(8) | 0.2128 | −0.2293 | 0.6398 | 0.12(3) |
| C3(8) | 0.0193 | 0.0969 | 0.6318 | 0.034(2) | H1(9) | −0.0174 | 0.3971 | 0.6939 | 0.09(3) |
| O4(8) | −0.0930 | 0.1044 | 0.6354 | 0.036(1) | H2(9) | 0.1917 | 0.5304 | 0.7083 | 0.09(3) |
| O5(8) | 0.1019 | 0.1704 | 0.6617 | 0.032(1) | H3(9) | 0.2374 | 0.2769 | 0.7323 | 0.06(2) |
| C1(9) | 0.0524 | 0.2780 | 0.7028 | 0.020(1) | H4(9) | 0.1288 | 0.4444 | 0.7623 | 0.18(5) |
| C2(9) | 0.1607 | 0.3910 | 0.7284 | 0.030(2) | H1(10) | −0.1714 | −0.1064 | 0.7863 | 0.14(4) |
| C3(9) | −0.0090 | 0.0984 | 0.7320 | 0.029(2) | H2(10) | −0.3143 | 0.1747 | 0.8095 | 0.18(5) |
| O4(9) | 0.0180 | −0.0910 | 0.7313 | 0.043(2) | H3(10) | −0.1946 | 0.3190 | 0.8380 | 0.05(2) |
| O5(9) | −0.0908 | 0.1757 | 0.7616 | 0.020(1) | H4(10) | −0.2474 | 0.0692 | 0.8606 | 0.04(2) |

| | +25 °C | | | | | +25 °C | | | |
|---|---|---|---|---|---|---|---|---|---|
| (b) | $x$ | $y$ | $z$ | $U_{eq}$/Å$^2$ | | $x$ | $y$ | $z$ | $U_{eq}$/Å$^2$ |
| C1(1) | 0.0495 | −0.2477 | −0.1119 | 0.098(8) | C1(10) | −0.1305 | 0.0461 | 0.7955 | 0.12(1) |
| C2(1) | 0.0316 | −0.4837 | −0.0968 | 0.12(1) | C2(10) | −0.2272 | 0.1569 | 0.8267 | 0.07(1) |
| C3(1) | 0.0317 | −0.0977 | −0.0703 | 0.081(5) | C3(10) | −0.0267 | −0.0030 | 0.8309 | 0.16(1) |
| O4(1) | −0.0592 | 0.0134 | −0.0655 | 0.083(4) | O4(10) | 0.0758 | 0.0763 | 0.8352 | 0.063(4) |


dx.doi.org/10.1021/ma2006624 |Macromolecules 2011, 44, 6441–6452

**Table 1. Continued**

| | +25 °C | | | | | +25 °C | | | |
|---|---|---|---|---|---|---|---|---|---|
| (b) | $x$ | $y$ | $z$ | $U_{eq}$/Å$^2$ | | $x$ | $y$ | $z$ | $U_{eq}$/Å$^2$ |
| O5(1) | 0.1377 | −0.0799 | −0.0476 | 0.109(3) | O5(10) | −0.0348 | −0.2006 | 0.8483 | 0.036(4) |
| C1(2) | 0.1351 | 0.0345 | −0.0034 | 0.076(3) | H1(1) | 0.1455 | −0.2331 | −0.1245 | 0.02(2) |
| C2(2) | 0.2682 | 0.0298 | 0.0162 | 0.142(4) | H2(1) | 0.0569 | −0.5971 | −0.1241 | 0.14(6) |
| C3(2) | 0.0309 | −0.0513 | 0.0280 | 0.049(3) | H3(1) | −0.065 | −0.5138 | −0.0874 | 0.05(3) |
| O4(2) | −0.0008 | −0.2357 | 0.0326 | 0.063(2) | H4(1) | 0.0889 | −0.5221 | −0.0668 | 0.05(3) |
| O5(2) | 0.0060 | 0.1178 | 0.0541 | 0.070(3) | H1(2) | 0.1148 | 0.2006 | −0.0139 | 0.05(3) |
| C1(3) | −0.0810 | 0.0549 | 0.0910 | 0.035(5) | H2(2) | 0.3374 | 0.0621 | −0.0102 | 0.16(6) |
| C2(3) | −0.1305 | 0.2647 | 0.1128 | 0.232(8) | H3(2) | 0.287 | −0.1298 | 0.0313 | 0.04(3) |
| C3(3) | −0.0262 | −0.0645 | 0.1330 | 0.058(3) | H4(2) | 0.2774 | 0.1501 | 0.0437 | 0.04(3) |
| O4(3) | 0.0849 | −0.0801 | 0.1356 | 0.127(5) | H1(3) | −0.1619 | −0.0348 | 0.0783 | 0.08(4) |
| O5(3) | −0.1035 | −0.1714 | 0.1599 | 0.068(3) | H2(3) | −0.1854 | 0.3547 | 0.0882 | 0.03(2) |
| C1(4) | −0.0472 | −0.2648 | 0.2016 | 0.257(9) | H3(3) | −0.0526 | 0.3664 | 0.124 | 0.08(4) |
| C2(4) | −0.1548 | −0.3908 | 0.2242 | 0.23(1) | H4(3) | −0.1883 | 0.2325 | 0.1432 | 0.23(10) |
| C3(4) | 0.0228 | −0.0812 | 0.2256 | 0.134(6) | H1(4) | 0.0184 | −0.3845 | 0.1878 | 0.03(3) |
| O4(4) | −0.0138 | 0.1021 | 0.2262 | 0.042(2) | H2(4) | −0.1965 | −0.5051 | 0.2001 | 0.12(6) |
| O5(4) | 0.0803 | −0.1847 | 0.2596 | 0.105(3) | H3(4) | −0.2266 | −0.2808 | 0.236 | 0.08(4) |
| C1(5) | 0.1281 | −0.0461 | 0.2968 | 0.058(6) | H4(4) | −0.1214 | −0.4822 | 0.2538 | 0.18(6) |
| C2(5) | 0.2319 | −0.1724 | 0.3220 | 0.127(6) | H1(5) | 0.1761 | 0.103 | 0.2857 | 0.08(4) |
| C3(5) | 0.0152 | 0.0273 | 0.3256 | 0.106(4) | H2(5) | 0.307 | −0.2119 | 0.3048 | 0.04(3) |
| O4(5) | −0.0728 | −0.0941 | 0.3257 | 0.102(5) | H3(5) | 0.1884 | −0.3161 | 0.341 | 0.05(3) |
| O5(5) | 0.0499 | 0.1836 | 0.3535 | 0.152(7) | H4(5) | 0.2654 | −0.0718 | 0.3562 | 0.04(3) |
| C1(6) | −0.0449 | 0.2530 | 0.3863 | 0.169(8) | H1(6) | −0.1389 | 0.2393 | 0.3725 | 0.09(4) |
| C2(6) | −0.0256 | 0.4852 | 0.4032 | 0.29(1) | H2(6) | −0.0328 | 0.6 | 0.3748 | 0.13(6) |
| C3(6) | −0.0288 | 0.1012 | 0.4278 | 0.025(5) | H3(6) | 0.0663 | 0.5026 | 0.4186 | 0.09(4) |
| O4(6) | 0.0537 | −0.0306 | 0.4292 | 0.125(4) | H4(6) | −0.0946 | 0.5291 | 0.4291 | 0.04(3) |
| O5(6) | −0.1316 | 0.0904 | 0.4522 | 0.109(4) | H1(7) | −0.1123 | −0.2016 | 0.4854 | 0.16(7) |
| C1(7) | −0.1346 | −0.0348 | 0.4952 | 0.146(5) | H2(7) | −0.3357 | −0.0832 | 0.4903 | 0.06(4) |
| C2(7) | −0.2662 | −0.0397 | 0.5163 | 0.141(8) | H3(7) | −0.2901 | 0.1191 | 0.5296 | 0.04(3) |
| C3(7) | −0.0375 | 0.0424 | 0.5307 | 0.060(5) | H4(7) | −0.272 | −0.156 | 0.5442 | 0.05(3) |
| O4(7) | 0.0079 | 0.2193 | 0.5282 | 0.047(3) | H1(8) | 0.1595 | 0.0404 | 0.5782 | 0.01(2) |
| O5(7) | 0.0003 | −0.1202 | 0.5569 | 0.077(6) | H2(8) | 0.1782 | −0.3576 | 0.5851 | 0.22(9) |
| C1(8) | 0.0810 | −0.0446 | 0.5942 | 0.28(1) | H3(8) | 0.0674 | −0.3556 | 0.63 | 0.04(3) |
| C2(8) | 0.1380 | −0.2566 | 0.6125 | 0.08(1) | H4(8) | 0.2128 | −0.2293 | 0.6377 | 0.12(5) |
| C3(8) | 0.0178 | 0.1075 | 0.6286 | 0.070(6) | H1(9) | −0.0174 | 0.3971 | 0.6919 | 0.09(4) |
| O4(8) | −0.0931 | 0.0815 | 0.6300 | 0.170(7) | H2(9) | 0.1917 | 0.5304 | 0.7062 | 0.10(4) |
| O5(8) | 0.0985 | 0.1721 | 0.6597 | 0.035(3) | H3(9) | 0.2374 | 0.2769 | 0.7302 | 0.06(3) |
| C1(9) | 0.0498 | 0.2734 | 0.7017 | 0.124(5) | H4(9) | 0.1288 | 0.4444 | 0.7602 | 0.19(8) |
| C2(9) | 0.1589 | 0.3898 | 0.7258 | 0.049(6) | H1(10) | −0.1714 | −0.1064 | 0.7842 | 0.11(6) |
| C3(9) | 0.0025 | 0.0985 | 0.7352 | 0.062(6) | H2(10) | −0.3143 | 0.1747 | 0.8074 | 0.20(8) |
| O4(9) | 0.0112 | −0.0938 | 0.7285 | 0.085(4) | H3(10) | −0.1946 | 0.319 | 0.8359 | 0.06(3) |
| O5(9) | −0.0952 | 0.1825 | 0.7562 | 0.122(4) | H4(10) | −0.2473 | 0.0692 | 0.8585 | 0.04(3) |

[a] $U_{(eqv)} = {}^1/_3\Sigma\Sigma[U_{ij}a^*_i a^*_j a_i a_j \cos(\tau_{ij})]$, where $U_{ij}$ is the component of anisotropic thermal parameter tensor. $a^*$ and $a$ are respectively the unit cell vectors of the reciprocal lattice and the real lattice. $\tau_{ij}$ is an angle between the vectors $a_i$ and $a_j$. [b] The numbering of the atoms is shown below. For example, C3(2) indicates the carbon atom of methyl group belonging to the 2nd monomeric unit in the repeating period. The H atoms were added to the carbon atoms at the standard geometries.

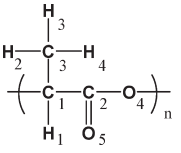



dx.doi.org/10.1021/ma2006624 |*Macromolecules* 2011, 44, 6441–6452

Table 2. Comparison of Skeletal Torsional Angles (degree) among the Various Structure Models of PLLA α Form: (a) −150 °C, (b) +25 °C, (c) a $2_1$ Helix, and (d) a Uniform (10/3) Helix[a]

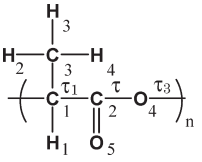

| | $\tau_1(1)$ | $\tau_2(1)$ | $\tau_3(1)$ | $\tau_1(2)$ | $\tau_2(2)$ | $\tau_3(2)$ | $\tau_1(3)$ | $\tau_2(3)$ | $\tau_3(3)$ | $\tau_1(4)$ |
|---|---|---|---|---|---|---|---|---|---|---|
| −150 °C | −158.9 | −177.9 | 62.3 | −156.7 | −174.9 | 72.8 | −170.0 | −169.9 | 59.3 | −164.1 |
| 25 °C | −151.2 | −172.3 | 50.2 | −153.3 | −172.1 | 79.1 | −162.2 | −174.6 | 51.9 | −173.7 |
| $2_1$ helix | −168.6 | −170.2 | 67.1 | −163.7 | −164.6 | 63.5 | −157.1 | −167.6 | 74.8 | −161.2 |
| uniform helix | −148.8 | −179.5 | 64.7 | −148.9 | −179.5 | 64.8 | −148.9 | −179.4 | 64.5 | −148.9 |

[a] $\tau_i(j)$ indicates the torsional angle $i$ of the $j$th monomeric unit. Only the torsional angles of the some limited monomer sequence are indicated here for simplicity. More detailed information is referred to in the Supporting Information.

needed to refine furthermore so as to give better reproduction for all the layer-line profiles of *hk*0, *hk*1, *hk*2, ..., and for the 00*L* reflection profile. Another point to be considered is about the disorder in the domain level. In the previous paper, we introduced an idea how to reproduce the observed 00*L* reflection profile for ethylene-tetrafluoroethylene alternating copolymer.[45] The X-ray structure analysis based on the *hkl* reflection data showed that the chains are packed regularly in the unit cell with the space group symmetry of $P\bar{1}$. This structure can reproduce the observed layer line profiles well, but not for a series of 00*L* reflections. Then we introduced a concept of domains with finite sizes, in which some unit cells are gathered together with keeping the regular packing structure of the chains. The relative height between the neighboring domains was shifted at random along the chain axis, giving a good reproduction of the observed 00*L* reflection profile. This idea of interdomain disorder may be applied to the present case of PLLA α form for explaining the relative intensities of the 00*L* reflections. The domains consisting of several unit cells were generated from Figure 4, and the relative heights of these domains were shifted randomly along the chain axis. (In this case, only the shift along the chain axis is important and so the domains were generated along the *a* axis only as an example.) The thus-constructed domain aggregation model was found to give the relatively good agreement of 00*L* reflection profile when compared with the observed data (see Figure 3). It should be noticed here that the layer line profiles shown in Figure 5 were not very much affected by this operation as long as the domains were enough large and keep the X-ray coherent condition.

**WAND Structure Analysis.** Figure 6a shows the observed 2D-WAND pattern taken at room temperature for the ultradrawn PLLA α form. In the X-ray structural analysis the hydrogen atoms were assumed to locate at the standard positions as described in the preceding section. The WAND data were applied to refine the positions and isotropic thermal parameters of hydrogen atoms by performing the least-squares calculation of WAND integrated intensities for the 92 reflections estimated in Figure 6a. In this refinement, the isotropic thermal parameters were assumed for the carbon and oxygen atoms and refined also. The final *R* factor was 23.0%. (The relatively high *R* value may come from the low signal-to-noise ratio of the observed reflection intensities and also the high background originated from the large contribution of incoherent scattering of the hydrogen atoms.) The thus-clarified atomic fractional coordinates and the corresponding isotropic thermal parameters are listed in Table 3. The WAND layer line profiles were calculated and compared with the observed ones in Figure 7. They give a relatively good agreement with the observed data although the signal-to-noise ($S/N$) ratio of the observed patterns is not very high. Figure 6b is the WAND pattern calculated by Cerius.[2] In parts c and d of Figure 6, the observed and calculated X-ray diffraction patterns are also shown for comparison, giving a good agreement with each other. In this way the crystal structure derived by the X-ray structure analysis has been established by the WAND analysis.

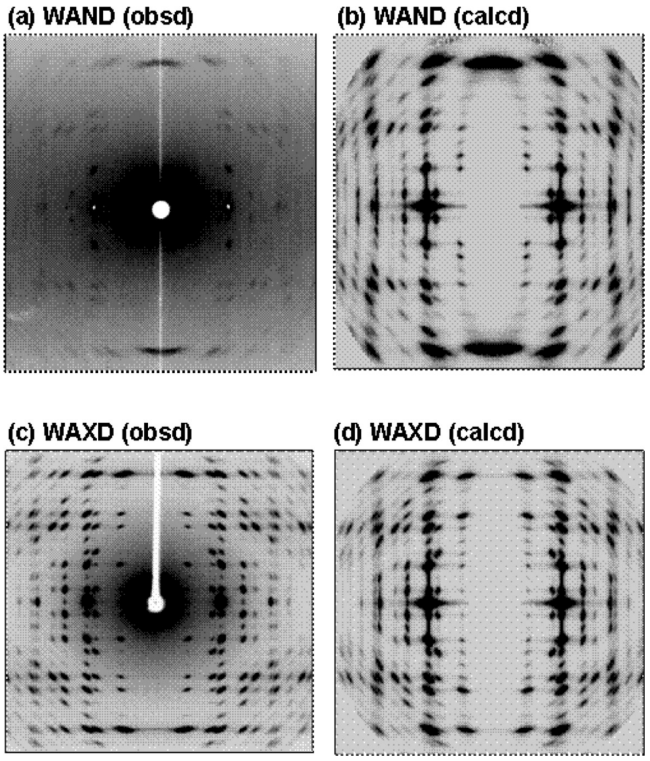


**Figure 6.** Wide-angle neutron diffraction diagram of PLLA α form (a) observed at 25 °C and (b) calculated by Cerius.[2] The X-ray diffraction diagram is also shown for comparison: (c) the diagram observed at 25 °C using synchrotron X-ray beam and (d) the calculated diagram.

**Table 3. Atomic Fractional Coordinates and Thermal Parameters of PLLA α Form Analyzed by WAND at 25 °C[a]**

| | $x$ | $y$ | $z$ | $U_{iso}$/Å$^2$ | | $x$ | $y$ | $z$ | $U_{iso}$/Å$^2$ |
|---|---|---|---|---|---|---|---|---|---|
| C1(1) | 0.0495 | −0.2477 | −0.1119 | 0.12(1) | C1(10) | −0.1305 | 0.0461 | 0.7955 | 0.12(1) |
| C2(1) | 0.0316 | −0.4837 | −0.0968 | 0.15(1) | C2(10) | −0.2272 | 0.1569 | 0.8267 | 0.081(7) |
| C3(1) | 0.0317 | −0.0977 | −0.0703 | 0.13(1) | C3(10) | −0.0267 | −0.0030 | 0.8309 | 0.068(7) |
| O4(1) | −0.0592 | 0.0134 | −0.0655 | 0.12(1) | O4(10) | 0.0758 | 0.0762 | 0.8352 | 0.10(1) |
| O5(1) | 0.1377 | −0.0799 | −0.0476 | 0.15(1) | O5(10) | −0.0348 | −0.2006 | 0.8483 | 0.18(2) |
| C1(2) | 0.1351 | 0.0345 | −0.0034 | 0.096(7) | H1(1) | 0.14(3) | −0.23(8) | −0.093(18) | 0.14(2) |
| C2(2) | 0.2682 | 0.0298 | 0.0162 | 0.30(2) | H2(1) | 0.068(14) | −0.593(8) | −0.124(3) | 0.05(2) |
| C3(2) | 0.0309 | −0.0513 | 0.0280 | 0.27(2) | H3(1) | −0.067(3) | −0.513(14) | −0.089(6) | 0.17(2) |
| O4(2) | −0.0008 | −0.2357 | 0.0326 | 0.09(1) | H4(1) | 0.085(13) | −0.512(11) | −0.065(3) | 0.09(2) |
| O5(2) | 0.0060 | 0.1178 | 0.0541 | 0.13(1) | H1(2) | 0.17(5) | 0.17(8) | −0.026(15) | 0.25(3) |
| C1(3) | −0.0810 | 0.0549 | 0.0910 | 0.100(8) | H2(2) | 0.336(4) | 0.05(7) | −0.012(2) | 0.18(2) |
| C2(3) | −0.1305 | 0.2646 | 0.1128 | 0.060(8) | H3(2) | 0.283(15) | −0.13(3) | 0.034(14) | 0.20(2) |
| C3(3) | −0.0262 | −0.0645 | 0.1330 | 0.21(1) | H4(2) | 0.280(14) | 0.16(5) | 0.041(12) | 0.22(3) |
| O4(3) | 0.0849 | −0.0801 | 0.1356 | 0.21(2) | H1(3) | −0.10(6) | −0.06(8) | 0.061(17) | 0.28(3) |
| O5(3) | −0.1035 | −0.1714 | 0.1599 | 0.18(1) | H2(3) | −0.16(2) | 0.373(16) | 0.0856(17) | 0.14(2) |
| C1(4) | −0.0472 | −0.2648 | 0.2016 | 0.074(8) | H3(3) | −0.054(7) | 0.34(2) | 0.132(7) | 0.02(1) |
| C2(4) | −0.1548 | −0.3908 | 0.2242 | 0.20(1) | H4(3) | −0.207(15) | 0.228(10) | 0.136(6) | 0.23(3) |
| C3(4) | 0.0228 | −0.0812 | 0.2256 | 0.25(2) | H1(4) | −0.02(4) | −0.39(6) | 0.175(11) | 0.16(2) |
| O4(4) | −0.0138 | 0.1021 | 0.2262 | 0.18(2) | H2(4) | −0.176(12) | −0.535(16) | 0.204(4) | 0.20(2) |
| O5(4) | 0.0803 | −0.1847 | 0.2596 | 0.19(2) | H3(4) | −0.237(6) | −0.288(12) | 0.227(6) | 0.01(1) |
| C1(5) | 0.1281 | −0.0461 | 0.2968 | 0.06(1) | H4(4) | −0.126(8) | −0.44(3) | 0.259(3) | 0.26(3) |
| C2(5) | 0.2319 | −0.1724 | 0.3220 | 0.064(8) | H1(5) | 0.17(4) | 0.06(9) | 0.270(14) | 0.28(3) |
| C3(5) | 0.0152 | 0.0273 | 0.3256 | 0.139(9) | H2(5) | 0.31(5) | −0.21(10) | 0.305(15) | 0.24(3) |
| O4(5) | −0.0728 | −0.0941 | 0.3257 | 0.30(2) | H3(5) | 0.19(6) | −0.32(7) | 0.341(18) | 0.18(2) |
| O5(5) | 0.0499 | 0.1836 | 0.3535 | 0.093(9) | H4(5) | 0.27(5) | −0.07(6) | 0.356(16) | 0.17(2) |
| C1(6) | −0.0450 | 0.2530 | 0.3863 | 0.13(1) | H1(6) | −0.10(4) | 0.26(3) | 0.354(9) | 0.01(1) |
| C2(6) | −0.0256 | 0.4852 | 0.4031 | 0.20(1) | H2(6) | −0.030(18) | 0.598(7) | 0.3739(16) | 0.16(2) |
| C3(6) | −0.0288 | 0.1012 | 0.4278 | 0.23(2) | H3(6) | 0.067(8) | 0.50(1) | 0.419(6) | 0.12(2) |
| O4(6) | 0.0537 | −0.0306 | 0.4292 | 0.12(1) | H4(6) | −0.096(11) | 0.53(1) | 0.429(5) | 0.02(1) |
| O5(6) | −0.1316 | 0.0904 | 0.4522 | 0.28(2) | H1(7) | −0.12(5) | −0.18(5) | 0.475(14) | 0.18(3) |
| C1(7) | −0.1346 | −0.0348 | 0.4952 | 0.17(1) | H2(7) | −0.335(4) | −0.09(3) | 0.490(2) | 0.32(4) |
| C2(7) | −0.2662 | −0.0397 | 0.5163 | 0.23(2) | H3(7) | −0.288(8) | 0.12(1) | 0.530(6) | 0.10(2) |
| C3(7) | −0.0375 | 0.0424 | 0.5307 | 0.15(1) | H4(7) | −0.267(7) | −0.16(2) | 0.545(4) | 0.08(1) |
| O4(7) | 0.0079 | 0.2193 | 0.5282 | 0.21(2) | H1(8) | 0.178(9) | 0.01(5) | 0.588(7) | 0.06(1) |
| O5(7) | 0.0003 | −0.1202 | 0.5569 | 0.12(1) | H2(8) | 0.231(12) | −0.33(5) | 0.606(7) | 0.03(1) |
| C1(8) | 0.0810 | −0.0446 | 0.5942 | 0.058(8) | H3(8) | 0.07(2) | −0.39(4) | 0.612(13) | 0.30(3) |
| C2(8) | 0.1380 | −0.2566 | 0.6125 | 0.19(2) | H4(8) | 0.14(2) | −0.18(6) | 0.647(6) | 0.18(2) |
| C3(8) | 0.0178 | 0.1074 | 0.6286 | 0.14(1) | H1(9) | −0.044(17) | 0.31(6) | 0.69(1) | 0.12(2) |
| O4(8) | −0.0931 | 0.0815 | 0.6300 | 0.17(1) | H2(9) | 0.19(2) | 0.52(3) | 0.704(6) | 0.15(2) |
| O5(8) | 0.0985 | 0.1721 | 0.6597 | 0.11(1) | H3(9) | 0.236(12) | 0.274(17) | 0.73(1) | 0.03(2) |
| C1(9) | 0.0498 | 0.2734 | 0.7017 | 0.12(1) | H4(9) | −0.21(2) | −0.06(5) | 0.80(1) | 0.12(2) |
| C2(9) | 0.1590 | 0.3898 | 0.7258 | 0.028(6) | H1(10) | 0.130(10) | 0.45(5) | 0.760(5) | 0.32(4) |
| C3(9) | 0.0025 | 0.0985 | 0.7352 | 0.17(1) | H2(10) | −0.316(5) | 0.17(3) | 0.808(3) | 0.22(3) |
| O4(9) | 0.0112 | −0.0938 | 0.7285 | 0.09(1) | H3(10) | −0.195(9) | 0.320(11) | 0.836(5) | 0.08(2) |
| O5(9) | −0.0952 | 0.1825 | 0.7562 | 0.08(1) | H4(10) | −0.242(12) | 0.063(16) | 0.858(3) | 0.08(1) |

[a] The numbering of the atoms is shown below. For example, C3(2) indicates the carbon atom of methyl group belonging to the 2nd monomeric unit in the repeating period. The fractional coordinates of C and O atoms are the same as those given in Table 1. The H atomic positions were refined by WAND analysis.

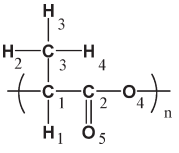



dx.doi.org/10.1021/ma2006624 |Macromolecules 2011, 44, 6441–6452

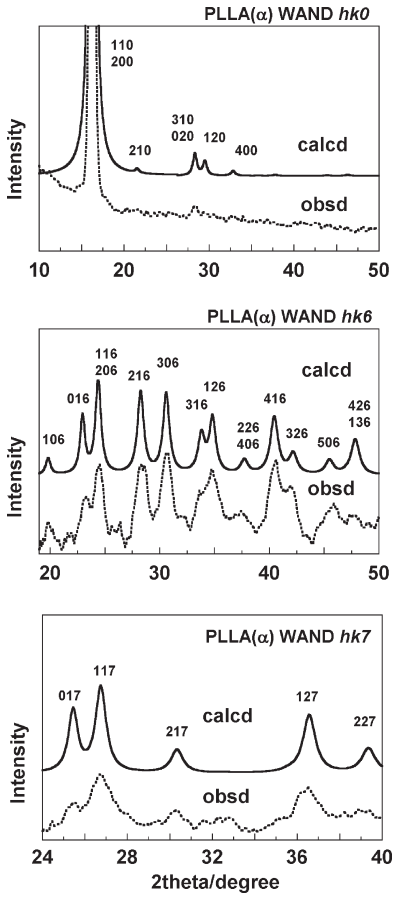


**Figure 7.** Comparison between the observed (dotted line) and calculated (solid line) wide-angle neutron diffraction profiles of PLLA α form for the several layer lines.

## CONCLUSION

The 2-dimensional WAXD patterns were measured at +25 °C and −150 °C for the ultradrawn PLLA α form by utilizing the high-energy synchrotron-sourced X-ray beam of short wavelength. The remarkably large number of X-ray reflections was successfully collected, which lead us to the derivation of an initial structural model by the direct method under the assumption of space group symmetry $P2_12_12_1$. This initial model was refined to obtain the accurate structure by performing the constrained least-squares calculation. The thus-obtained structure model was essentially the same as that reported by Sasaki et al.[19] and gave a relatively good agreement between the observed and calculated integrated intensities. But, the layer line profiles were not reproduced enough well by using this $2_1$-helical model. The observed odd-numbered 00*l* reflections required us to eliminate the chain conformation of $2_1$ screw symmetry. These observations might be ascribed to the slight disorder in chain packing mode,[19] but our calculation of 00*L* reflection intensities by introducing the chain packing disorder did not give any odd-numbered reflections as long as the molecular chains keep the $2_1$ helical symmetry rigidly. We needed to reduce the chain symmetry furthermore. As a tentative model of the reduced symmetry, the monoclinic type unit cell of $P12_11$ space group was assumed to keep the relationship between the adjacent upward and downward chains, and the structure was refined furthermore. The 10 monomeric units included in the fiber period were symmetrically independent. The finally obtained model gave the *R* factor of 19.3% for about 700 reflections at −150 °C and 19.4% for about 550 reflections at 25 °C. All of the observed layer line profiles were reproduced also excellently. The thus obtained structure was transferred to the calculation of WAND pattern, and the hydrogen atomic positions were refined to give the lowest *R* factor of 23.0%. The observed WAND layer line profiles were reproduced well in addition to the relatively good reproduction of the observed layer line profiles. It is noticed here that, although the deviation from the uniform (10/3) helical conformation and the loss of $2_1$ screw symmetry are not very significant as seen from the small changes in the skeletal torsional angles for example, the totally nonsymmetric chain form can reproduce the observed data including the 2-D X-ray diffraction pattern, the layer line profiles and the 2-D neutron diffraction data consistently.

The crystal structure of PLLA α form has been established in this way on the basis of the 2-dimensional diffraction patterns taken with the quantum beams or the synchrotron high-energy X-ray beam and neutron beam. This structure may allow us to estimate the ultimate elastic and compliance constants of the α crystal form theoretically using a lattice dynamic method.[39−42] The concrete calculation results will be reported separately.

## ASSOCIATED CONTENT

**Supporting Information.** Comparison of observed and calculated structure factors of PLLA. This material is available free of charge via the Internet at http://pubs.acs.org.

## ACKNOWLEDGMENT

This study was performed under the financial support by "the Strategic Project to Support the Formation of Research Base at Private University (2010-2014)" of the Ministry of Education, Science, Culture and Sports, Japan.

## REFERENCES

(1) Auras, R.; Harte, B.; Selke, S. *Macromol Biosci.* **2004**, *4*, 835.
(2) Nishino, T. *Polym. Prepr. Jpn* **2000**, *49*, 4345.
(3) Kanamoto, T.; Furukawa, T.; Sawai, D.; Hyon, S.-H.; Sungil, M. *Fiber Prepr. Jpn.* **2006**, *1*, 43.
(4) Montes de Oca, H.; Ward, I. M. J. *J. Polym. Sci., Part B: Polym. Phys.* **2007**, *45*, 892.
(5) Born, M.; Huang, K. *Dynamical Theory of Crystal Lattice*; Oxford University Press: London, 1954.
(6) Tashiro, K. *Prog. Polym. Sci.* **1993**, *18*, 377.
(7) Eling, B.; Gogolewski, S.; Pennings, A. J. *Polymer* **1982**, *23*, 1587.
(8) Zhang, J.; Duan, Y.; Sato, H.; Tsuji, H.; Noda, I.; Yan, S.; Ozaki, Y. *Macromolecule* **2005**, *38*, 8012.
(9) Puiggali, J.; Ikada, Y.; Tsuji, H.; Cartier, L.; Okihara, T.; Lotz, B. *Polymer* **2000**, *41*, 8921.
(10) Cartier, L.; Okihara, T.; Ikada, Y.; Tsuji, H.; Puiggali, J.; Lotz, B. *Polymer* **2000**, *41*, 8909.
(11) Ikada, Y.; Jamshidi, K.; Tsuji, H.; Hyon, S.-H. *Macromolecules* **1987**, *20*, 904.
(12) De Santis, P.; Kovacs, J. *Biopolymers* **1968**, *6*, 299.
(13) Brant, A. D.; Tonelli, A. E.; Flory, P. J. *Macromolecules* **1969**, *2*, 228.
(14) Okihara, T.; Tsuji, M.; Kawaguchi, A.; Katayama, K. *J. Macromol, Sci. Phys. B.* **1991**, *30*, 119.
(15) Kobayashi, J.; Asahi, T.; Ichiki, M.; Okikawa, A.; Suzuki, H.; Watanabe, T.; Fukada, E.; Shikinami, Y. *J. Appl. Phys.* **1995**, *77*, 2957.
(16) Hoogsteen, W.; Postema, A. R.; Pennings, A. J.; ten Brinke, G.; Zugenmaier, P. *Macromolecules* **1990**, *23*, 634.

(17) Alemán, C.; Lotz, B.; Puiggali, J. *Macromolecules* **2001**, *34*, 4795.
(18) Kang, S.; Hsu, S. L.; Stidman, H. D.; Smith, P. B.; Leugers, M. A.; Yang, X. *Macromolecule* **2001**, *34*, 4542.
(19) Sasaki, S.; Asakura, T. *Macromolecules* **2003**, *23*, 8385.
(20) Sawai, D.; Takahashi, K.; Imamura, T.; Nakamura, K.; Kanamoto, T.; Hyon, S.-H. *Polym. Sci.: Part B: Polym. Phys.* **2002**, *40*, 95.
(21) Stout, G. H.; Jensen, L. H. *X-ray Structure Determination: A Practical Guide*, 2nd ed.; John Wiley & Sons: New York, 1989.
(22) Tadokoro, H. *Structure of Crystalline Polymers*; John Wiley & Sons: New York, 1990.
(23) Alexander, L. L. *X-ray Diffraction Methods in Polymer Science*; John Wiley & Sons: New York, 1969.
(24) Tashiro, K.; Anasaga, H.; Ishino, K.; Tazaki, R.; Kobayashi, M. *J. Polym. Sci., Part B: Polym. Phys.* **1997**, *35*, 1677.
(25) Tashiro, K.; Hanesaka, M.; Ohhara, T.; Ozeki, T.; Kitano, T.; Nishu, T.; Kurihara, K.; Tamada, T.; Kuroki, R.; Fujiwara, S.; Tanaka, I.; Niimura, N. *Polym. J.* **2007**, *39*, 1253.
(26) Tashiro, K.; Hanesaka, M.; Ozeki, T. *Polym. Prepr. Jpn.* **2008**, *57*, 734.
(27) Busing, W. R. *Macromolecules* **1990**, *23*, 4608.
(28) Hanesaka, M. *Hamon (Jpn. Soc. Neutron Sci.)* **2009**, *19*, 26.
(29) Tashiro, K.; Tanaka, I.; Oohara, T.; Niimura, N.; Fujiwara, S.; Kamae, T. *Macromolecules* **2004**, *37*, 4109.
(30) Hanesaka, M.; Tashiro, K.; Ohhara, T.; Kurihara, K.; Kuroki, R.; Tamada, T.; Tanaka, I.; Niimura, N.; Kitano, T.; Nishu, T.; Katsube, K.; Morikawa, K.; Komiya, Y. *Polym. Prepr. Jpn* **2008**, *57*, 3734.
(31) Hanesaka, M.; Tashiro, K.; Yoshizawa, Y.; Hirayama, R.; Kitano, T.; Nishu, T.; Ohhara, T.; Kuroki, R.; Tamada, T.; Kurihara, K.; Tanaka, I.; Niimura, N. *Polym. Prepr. Jpn.* **2007**, *56*, 4010.
(32) Tashiro, K.; Hanesaka, M.; Ohhara, T.; Kurihara, K.; Kuroki, R.; Tamada, T.; Fujiwara, S.; Katsube, K.; Morikawa, K.; Komiya, Y. *Polym. Prepr. Jpn* **2009**, *58*, 3539.
(33) Wilson, C. C. *Single Crystal Neutron Diffraction from Molecular Materials*; World Scientific Publ. Co.: Singapore, 2000.
(34) Niimura, N.; Karasawa, Y.; Tanaka, I.; Miyahara, J.; Akahashi, K.; Saito, H.; Koizumi, S.; Hidaka, M. *Nucl. Instrum. Methods* **1994**, *A349*, 521.
(35) http://www.acnr.nist.gov./instruments/bt1/neutron.html
(36) Farragia, L. J. *J. Appl. Crystallogr.* **1999**, *32*, 837.
(37) Sheldrick, G. M. *Acta Crystallogr.* **1990**, *A46*, 467.
(38) Sheldrick, G. M. *SHELXL-97 - A program for Crystal Structure Refinement*; University of Gottingen: Gottingen, Germany, 1997; Release 97−2.
(39) Takahashi, Y.; Tadokoro, H. *Macromolecules* **1973**, *6*, 672.
(40) Huggins, M. L. *J. Chem. Phys.* **1945**, *13*, 37.
(41) Uchida, T.; Tadokoro, H. *J. Polym. Sci., Part A-2* **1967**, *5*, 63.
(42) Carazzolo, G. A. *J. Polym. Sci., Part A* **1963**, *1*, 1573.
(43) Takahashi, Y.; Tadokoro, H. *J. Polym. Sci., Polym. Phys. Ed.* **1978**, *6*, 1219.
(44) Saruyama, Y.; Miyaji, H.; Asai, K. *J. Polym. Sci., Polym. Phys. Ed.* **1978**, *17*, 1163.
(45) Funaki, A.; Phongtamrug, S.; Tashiro, K. *Macromolecules* **2011**, *44*, 1540.